

# Voltage Stability Enhancement Through Active Power Control of Converter-Interfaced Generation

Weilin Zhong, Federico Milano  
School of Electrical & Electronic Engineering  
UCD  
Dublin, Ireland

Georgios Tzounas  
Power Systems Laboratory  
ETH  
Zürich, Switzerland

**Abstract**—The paper investigates the ability of Converter-Interfaced Generators (CIGs) to improve the stability margin of power systems by adjusting their active power injections at their points of connection. To this aim, a voltage magnitude-active power control scheme is examined and its effectiveness is tested considering different topology and CIG reactive power capability scenarios. The focus is on the effect on long-term voltage instabilities due to the system reaching its loadability limit, as well as on small-disturbance, short-term instabilities, arising in the form of Hopf bifurcations. Simulation results are based on a continuation power flow analysis carried out considering a modified version of the IEEE 39-bus system, where a portion of synchronous machines is replaced by CIGs.

**Index Terms**—Active/reactive power regulation, Converter-Interfaced Generators (CIGs), voltage control, loadability margin, Hopf bifurcation.

## I. INTRODUCTION

The increasing penetration of Converter-Interfaced Generators (CIGs) leads to higher levels of uncertainty, and changes the conventional flows of the power from remote generation to load centers, which in turn impact on the overall voltage profile and loadability margin of the system. On the other hand, CIG controls can be employed to provide a variety of beneficial services and, if properly designed and coordinated, they can also contribute in enhancing power system stability [1]. This paper elaborates on CIG controls and proposes a scheme to regulate the voltage by exploiting their active power capabilities.

Voltage instability has been the cause of many power black-outs worldwide and is thus considered a major threat to power system secure operation [2]. In recent years, a number of works have examined the impact of CIGs on voltage stability as well as the potential of effectively utilizing their control capabilities to provide proper corrective actions and prevent a voltage collapse, e.g. see [3]–[6]. With this regard, voltage regulation through appropriate management of reactive power reserves is currently considered the primary countermeasure against voltage instabilities. However, researchers have also emphasized that keeping constant voltages through CIGs

integrated in distribution networks needs to be done carefully, otherwise it may lead to a delayed detection of an imminent instability, see [6].

Available power from renewable resources, such as wind and solar, are currently not fully utilized in the power system. For example, in the Irish transmission system, 12.1% of the total available wind energy in 2020 was *dispatch-down*<sup>1</sup> [7], [8]. Part of this energy could be potentially utilized for voltage regulation. As a matter of fact, some recent studies have explored the potential of providing voltage regulation through active power management [9]–[11]. The rationale behind these references is that, at the distribution level, where CIGs are often connected, the interaction between voltage magnitude and active power variations is considerable. In this vein, an active power-based voltage control scheme for improved synchronization and power sharing of low-voltage microgrids is discussed in [9]. The authors in [10] propose an optimal control strategy to improve long-term voltage stability through both active and reactive power compensation provided by a battery energy storage system. Finally, a control scheme in which both active and reactive power of distributed energy resources are varied to provide both primary frequency and voltage regulation is proposed in [11].

This paper proposes an active power-based voltage control approach for CIGs. The approach consists in controlling the voltage by means of both the active and reactive power injections to the grid. The performance of the proposed control in improving the stability margin of power systems is tested with a comprehensive case study based on a continuation power flow analysis. The impacts on long-term voltage stability margin, as well as on short-term, small-signal stability margin, are evaluated.

The remainder of the paper is organized as follows. Section II provides a theoretical background on the relationship between bus voltages and power injections in a power network. Section III describes the structure of the CIG voltage control model utilized in this paper. Section IV discusses the simulation results obtained based on a modified version of the IEEE 39-bus system. Finally, conclusions are drawn and future work directions are outlined in Section V.

This work was supported by the European Commission, by funding W. Zhong and F. Milano under the project EdgeFLEX, grant agreement no. 883710; by the Swiss National Science Foundation, by funding G. Tzounas under the NCCR Automation project (grant no. 51NF40 18054); and by Sustainable Energy Authority of Ireland (SEAI), by funding F. Milano under the project FRESLIPS, grant agreement no. RDD/00681.

<sup>1</sup>The expression *wind dispatch-down* refers to the available wind energy that is not allowed in the grid due to local network constraints and/or system-wide security issues.

## II. THEORETICAL BACKGROUND

This section provides a qualitative appraisal on the link between bus voltages and active/reactive power injections in a power network. This serves as the theoretical motivation of the approach proposed in the paper.

The active and reactive power injections  $p_h$  and  $q_h$  at bus  $h$  of a network with  $n$  buses are given by the well-known power flow equations:

$$\begin{aligned} p_h &= \sum_{k=1}^n v_h v_k [G_{hk} \cos \theta_{hk} + B_{hk} \sin \theta_{hk}], \\ q_h &= \sum_{k=1}^n v_h v_k [G_{hk} \sin \theta_{hk} - B_{hk} \cos \theta_{hk}], \end{aligned} \quad (1)$$

where  $G_{hk}$  and  $B_{hk}$  are the real and imaginary parts of the  $(h, k)$  element of the network's admittance matrix  $\mathbf{Y} \in \mathbb{C}^{n \times n}$ ;  $v_h, v_k$  are the voltage magnitudes at buses  $h, k$ , respectively; and  $\theta_{hk} = \theta_h - \theta_k$ , where  $\theta_h$  and  $\theta_k$  are the voltage phase angles at buses  $h$  and  $k$ , respectively.

Consider that a CIG is connected to the power network radially, as shown in Fig. 1. The parameters  $R_{hk}$  and  $X_{hk}$  denote the real and imaginary parts of the  $(h, k)$  element of the corresponding impedance matrix  $\mathbf{Z} \in \mathbb{C}^{n \times n}$ , where  $\mathbf{Z}$  is the inverse of  $\mathbf{Y}$ . Note that, for simplicity but without lack of generality, in this section, we do not consider the capacitive charging of the lines.

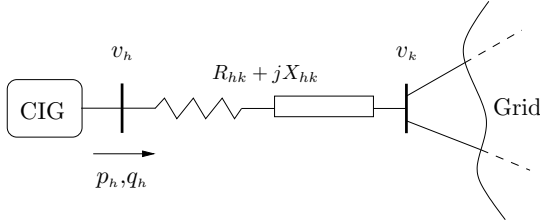


Fig. 1: CIG connected in antenna to the grid.

According to equations (1), the bus voltage magnitude  $v_h$  is, in general, a function of both  $q_h$  and  $p_h$ . Here we are particularly interested in the interaction between  $v_h$  and the active power injection  $p_h$  and in discussing how this interaction varies depending on the resistance/inductance ratio of the network to which the CIG is connected. To this aim, we consider two extreme cases for the feeder that connects the CIG to the network, namely, purely inductive and purely resistive.

A purely inductive feeder ( $R_{hk} \approx 0$ ) implies that the CIG is connected at the high-voltage transmission level, where the resistance/inductance ratio is typically very small ( $R_{hk}/X_{hk} \ll 1$ ). In this case, (1) takes the form:

$$\begin{aligned} p_h &= \frac{v_h v_k}{X_{hk}} \sin \theta_{hk}, \\ q_h &= \frac{v_h^2}{X_{hk}} - \frac{v_h v_k}{X_{hk}} \cos \theta_{hk}, \end{aligned} \quad (2)$$

or, equivalently:

$$\frac{v_h^2 v_k^2}{X_{hk}^2} = p_h^2 + \left( q_h - \frac{v_h^2}{X_{hk}} \right)^2, \quad (3)$$

or, equivalently:

$$0 = v_h^4 - (2q_h X_{hk} + v_k^2) v_h^2 + (p_h^2 + q_h^2) X_{hk}^2. \quad (4)$$

Equation (4) is a second-order equation with respect to  $v_h^2$ . Solution for  $v_h$  gives:<sup>2</sup>

$$v_h = \sqrt{q_h X_{hk} + \frac{v_k^2}{2} \pm \sqrt{\frac{v_k^4}{4} + q_h X_{hk} v_k^2 - p_h^2 X_{hk}^2}}. \quad (5)$$

On the other hand, a purely resistive feeder ( $X_{hk} \approx 0$ ) implies that the CIG is connected at a low-voltage network. In this case, (1) becomes:

$$\begin{aligned} p_h &= \frac{v_h^2}{R_{hk}} + \frac{v_h v_k}{R_{hk}} \cos \theta_{hk}, \\ q_h &= \frac{v_h v_k}{R_{hk}} \sin \theta_{hk}, \end{aligned} \quad (6)$$

and, through the same steps as those that lead to (5), we obtain the following expression for  $v_h$ :

$$v_h = \sqrt{p_h R_{hk} + \frac{v_k^2}{2} \pm \sqrt{\frac{v_k^4}{4} + p_h R_{hk} v_k^2 - q_h^2 R_{hk}^2}}. \quad (7)$$

Expressions (5) and (7) are obtained, of course, for limit cases and, of course, do not represent a physical connection. However, they indicate that the higher the resistance, the more  $v_h$  is affected (and thus can be regulated) by  $p_h$ . This is the first property that we exploit in the remainder of this work.

We have discussed so far that the voltage is sensitive to active power injections. This fact *per se* does not imply that regulating the voltage through the active power will necessarily increase the maximum transfer capability of a grid. However, we observe that, in general, CIGs are distributed in the grid and are typically closer to the loads than conventional large power plants. Thus, one has to expect that using CIGs to compensate the increase of the load power consumption will, overall, reduce the power transmission in the transmission lines. This reduction has to be expected to be more effective if not only the reactive power but also the active one is regulated to support the voltage. This is the second property that we exploit in the remainder of this paper.

## III. CONTROL STRUCTURE

This section describes the basic control structure of a CIG model that employs standard filters and controllers widely used in industrial applications. This model is then utilized in the case study presented in Section IV.

The block diagram of the CIG controller is depicted in Fig. 2. It consists of: (i) an inner control loop that regulates the components ( $i_d, i_q$ ) of the current in the dq reference frame, (ii) a voltage control loop that adjusts the bus voltage error

<sup>2</sup>Existence of real solutions requires a non-negative discriminant, in this case  $\frac{v_k^4}{4} + q_h X_{hk} v_k^2 - p_h^2 X_{hk}^2 \geq 0$ .

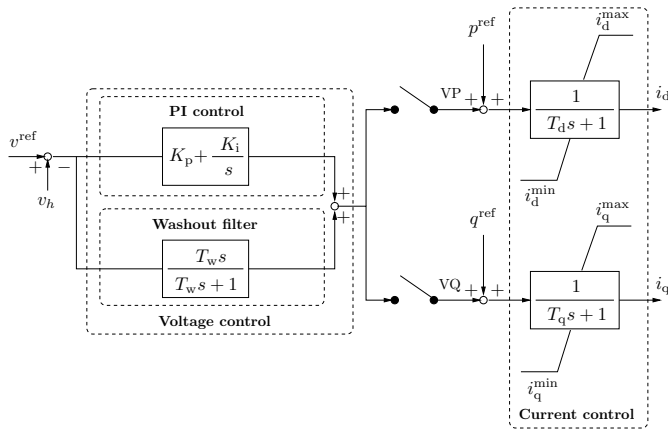


Fig. 2: CIG voltage control diagram.

$v^{\text{ref}} - v_h$  through a Proportional-Integral (PI) and a washout filter connected in parallel.  $p^{\text{ref}}$  and  $q^{\text{ref}}$  are the CIG's active and reactive power references, respectively.

In conventional power systems, bus voltages are typically regulated through variation of the available reactive power ( $V$ - $Q$  control). In Fig. 2 and in the remainder of the paper, the  $V$ - $Q$  control strategy is denoted with  $VQ$ . In order to evaluate the ability of CIGs to enhance the system's stability by properly modifying their active power injections, an additional channel that regulates the voltage by modifying the active power reference, namely  $VP$ , is employed in the CIG controller (see Fig. 2). The resulting CIG control strategy will be referred to as  $VQ+VP$  control.

#### IV. CASE STUDY

In this section, we carry out numerical simulations to evaluate the ability of CIGs to improve the stability margin of power systems through the proposed  $VQ+VP$  control scheme. To this aim, a modified version of the IEEE 39-bus system is considered. Simulation results are obtained using the power system analysis software tool Dome [12].

The single-line diagram of the examined test system is shown in Fig. 3. For all scenarios, Synchronous Machines (SMs) are modeled with a 4-th order (two-axis) model and are equipped with turbine governors, automatic voltage regulators, and power system stabilizers; loads are modeled as constant power consumption [13]. The modifications with respect to the original system are the following: the SMs at buses 30, 37 and 38 have been replaced by CIGs, the voltage controllers of which are represented using the model described in Section III. The parameters utilized for the CIG inner current and voltage controls are given in Table I. With the above changes, 30% of the system's power generation is provided by CIGs.

A continuation power flow analysis is carried out by stressing the system through variation of a scalar loading parameter  $\mu$  that multiplies all generator and load powers. The continuation power flow routine is setup to check at each point for the occurrence of Hopf bifurcations, since saddle node bifurcations are often preceded by a small-signal instability

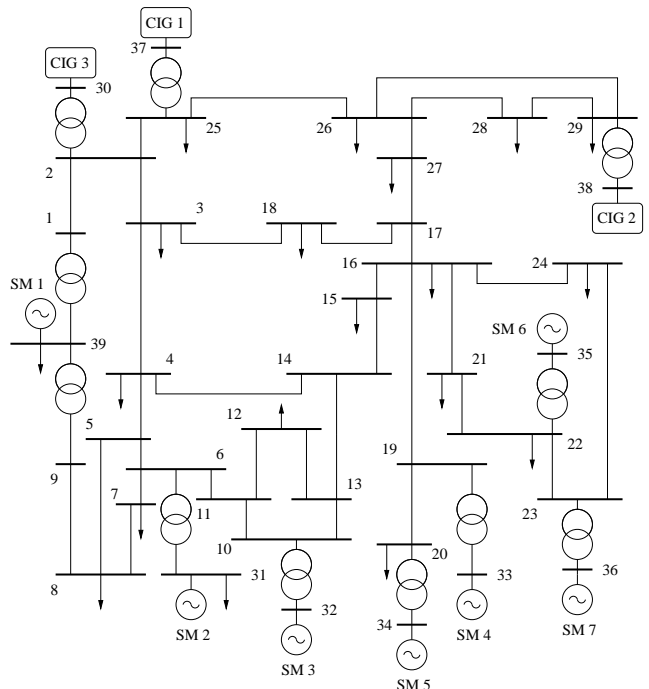


Fig. 3: Modified IEEE 39-bus system.

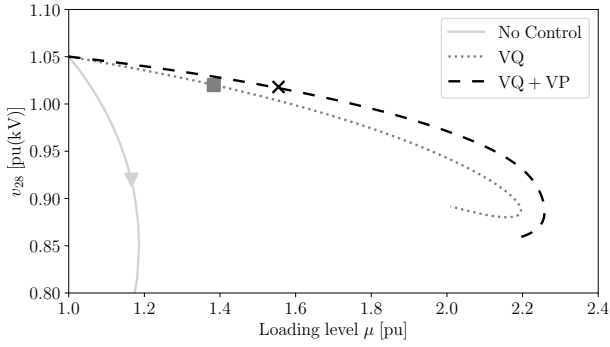
TABLE I: Parameters of CIG controls.

Control	Parameters
Current	$T_d = 0.04$ s, $T_q = 0.04$ s
Voltage	$K_p = 10$ , $K_i = 5$ , $T_w = 0.1$ s

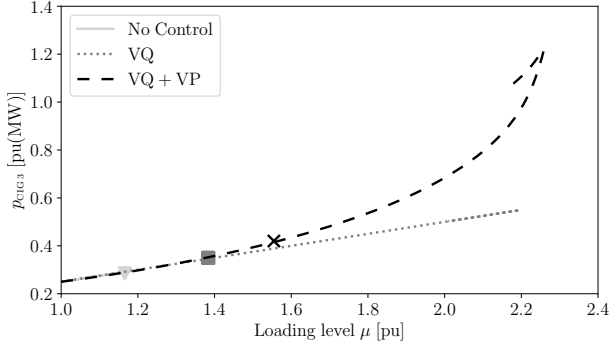
[14]. The  $VQ+VP$  control is compared to the  $VQ$  control, as well as to the scenario in which the CIGs do not provide voltage control. In the plots, the Hopf bifurcation points for the three CIG control scenarios, namely, no voltage control, classic  $VQ$  control, and  $VQ+VP$  control, are denoted with  $\nabla$ ,  $\blacksquare$  and  $\times$ , respectively.

The voltage at load bus 28 and the active and reactive power outputs of CIG 3 as the loading level  $\mu$  of the system is increased, are presented in Fig. 4. Results show that the stability margin of the system for each of the examined scenarios is given by the respective Hopf bifurcation point. The  $VQ+VP$  control provides a significant improvement to the system's stability margin (see Fig. 4a). Moreover, this improvement is achieved without a need for large variation of the CIG's active power generation (see Fig. 4b). The latter point is very important if a  $VQ+VP$  control is to be implemented in practice, where CIGs often operate with limited active power reserves [7], [8]. Finally, it is worth noting that the  $VQ+VP$  control improves the stability margin even if generator and controller dynamics were not taken into account. This is shown in Fig. 4a, where the saddle node for the  $VQ+VP$  control is encountered for a loading level that is higher compared to the no control and  $VQ$  control scenarios.

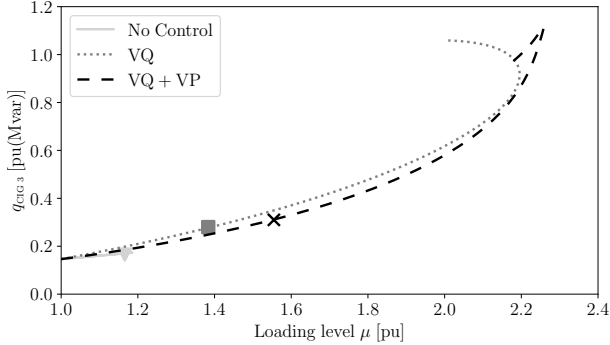
It is relevant to note that similar results can be obtained



(a) Loading level-voltage curve at bus 28.



(b) Loading level-active power curve for CIG 3.

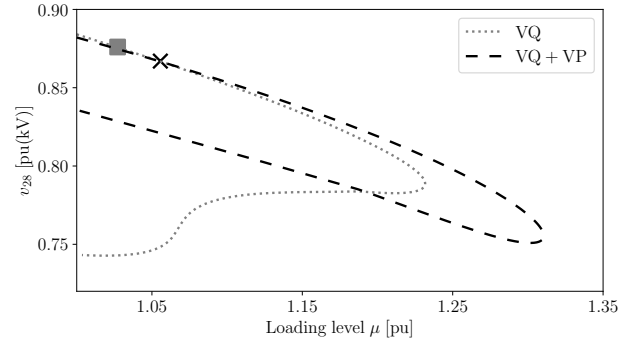


(c) Loading level-reactive power curve for CIG 3.

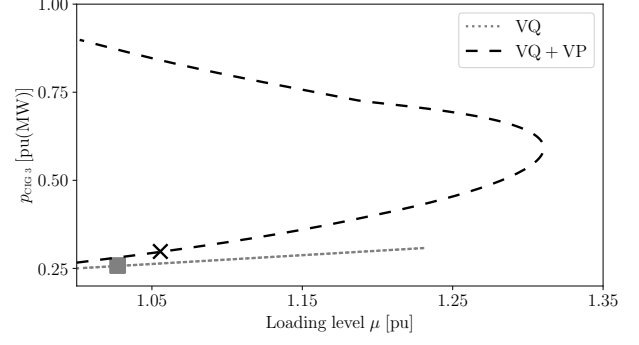
Fig. 4: Comparison of control modes.

by considering that multiple resources are integrated at the distribution level and connected to the transmission system through a Under-Load Tap Changer (ULTC) transformer. For the sake of example, we also carried out a simulation where the CIGs are substituted by distribution networks that comprise a cluster of devices, including renewable sources, storage systems, and dispatchable loads. The topology of the distribution network used in that exercise is the same as the one considered in [15]. Results confirm the above expectation, i.e. that the VQ+VP control provided by multiple resources integrated within the distribution system and connected to the high-voltage through a ULTC transformer, is able to significantly improve the stability margin of the system.

Next, we validate the performance of the proposed controller when employed in a high  $R/X$  network. With this aim, the line resistances in the modified 39-bus system are increased to be in the same order of magnitude with the line reactances.



(a) Loading level-voltage curve at bus 28.



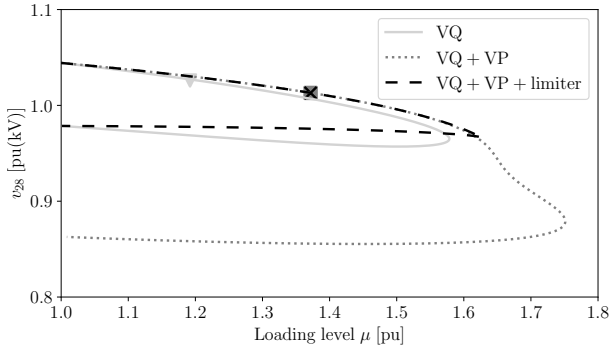
(b) Loading level-active power curve for CIG 3.

Fig. 5: Comparison of control modes,  $R \approx X$ .

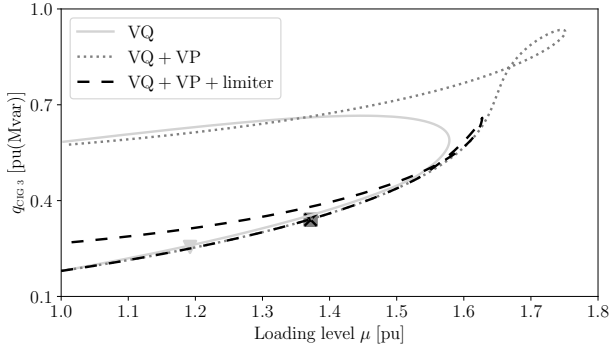
In this case, the loading level-voltage curve at load bus 28 and the loading level-active power curve for CIG 3 are shown in Fig. 5. As expected, the controller improves the voltage stability margin more significantly in a high  $R/X$  network than in a low  $R/X$  network (see saddle nodes in Fig. 5.a). This result is consistent with the discussion in Section II, and in particular with (7) and confirms the expectation that, in a resistive network, the voltage has stronger sensitivity with respect to the active power than the reactive one. It is also relevant to observe that the Hopf bifurcation occurs at a lower loading level for the  $R \approx X$  system. This happens because the increased  $R/X$  ratio changes the line impedance factor, for which the Hopf bifurcation conditions are affected, and thus unstable voltage oscillations are introduced by the SM automatic voltage regulators [16], [17].

A relevant remark is that the reactive power of CIGs might be limited by the line impedance. In this vein, we further evaluate the suitability of the proposed controller under limited reactive power generation. Figure 6 shows that the reactive power limits compromise the performance of the VQ+VP controller, and the maximum loading level is met at the point where the reactive power output of the CIG reaches its maximum. However, compared to the conventional VQ control mode, the limited VQ+VP control still provides a higher stability margin.

A summary of the results obtained for different contingencies and control modes is finally presented in Table II, where  $\mu_{HB}$  refers to the Hopf bifurcation of the system and  $\mu_{max}$  refers to the loading level for which the saddle-node



(a) Loading level-voltage curve at bus 28.



(b) Loading level-reactive power curve for CIG 3.

Fig. 6: Effect of reactive power limit.

bifurcation is met. The results are presented in Table II and suggest that, overall, the proposed VQ+VP control yields an improvement both in the short-term and long-term stability margin of the system examined. In particular, it provides a stability margin improvement of about 15-20% over the classic voltage-reactive power controller.

TABLE II: Loading level at Hopf bifurcation  $\mu_{HB}$  and maximum continuation parameter  $\mu_{max}$  for different  $N - 1$  contingencies and control modes.

Parameters	$\mu_{HB}$		$\mu_{max}$	
	VQ	VQ + VP	VQ	VQ + VP
N/A	1.3835	<b>1.5547</b>	2.1956	<b>2.2584</b>
SM 2 out.	1.0000	<b>1.0352</b>	1.7894	<b>1.8542</b>
SM 3 out.	1.2478	<b>1.4764</b>	1.8296	<b>1.8964</b>
SM 5 out.	1.3593	<b>1.5299</b>	2.0226	<b>2.1125</b>
SM 6 out.	1.2810	<b>1.4794</b>	2.0034	<b>2.0289</b>
Line 4-5 out.	1.3273	<b>1.5159</b>	2.1566	<b>2.2127</b>
Line 14-15 out.	1.3556	<b>1.5383</b>	2.1724	<b>2.2294</b>
Line 21-22 out.	1.1920	<b>1.3717</b>	1.5785	<b>1.7512</b>
Line 26-29 out.	1.3716	<b>1.5397</b>	2.1586	<b>2.2299</b>

## V. CONCLUSIONS

This paper proposes an approach to improve stability of power systems through active power control of CIGs. A continuation power flow analysis is carried out considering the effect of different contingencies and network characteristics

to evaluate the performance of the proposed control method. Results indicate that with the proposed control, both Hopf and saddle node bifurcations are encountered at higher loading levels compared to the standard voltage-reactive control approach.

Future work will focus on implementing a more detailed control design based on the proposed approach, as well as testing its robustness under different disturbances in transient conditions.

## REFERENCES

- [1] N. Hatziaargyriou *et al.*, "Contribution to bulk system control and stability by distributed energy resources connected at distribution network," IEEE, Tech. Rep., 2017.
- [2] H. Haes Alhelou, M. E. Hamedani-Golshan, T. C. Njenda, and P. Siano, "A survey on power system blackout and cascading events: Research motivations and challenges," *Energies*, vol. 12, no. 4, p. 682, 2019.
- [3] J. W. Simpson-Porco, Q. Shafiee, F. Dörfler, J. C. Vasquez, J. M. Guerrero, and F. Bullo, "Secondary frequency and voltage control of islanded microgrids via distributed averaging," *IEEE Transactions on Industrial Electronics*, vol. 62, no. 11, pp. 7025–7038, 2015.
- [4] T. Souxes, G. Tzounas, and C. Vournas, "Effect of wind variability in the emergency reactive support provided by wind farms," in *2017 IEEE Manchester PowerTech*. IEEE, 2017, pp. 1–6.
- [5] M. N. I. Sarkar, L. G. Meegahapola, and M. Datta, "Reactive power management in renewable rich power grids: A review of grid-codes, renewable generators, support devices, control strategies and optimization algorithms," *IEEE Access*, vol. 6, pp. 41 458–41 489, 2018.
- [6] P. Mandoulidis, T. Souxes, and C. Vournas, "Impact of converter interfaced generators on power system long-term voltage stability monitoring and control," *Electric Power Systems Research*, vol. 199, p. 107438, 2021.
- [7] EirGrid and SONI, "Annual Renewable Energy Constraint and Curtailment Report 2020," URL: <https://www.eirgridgroup.com/site-files/library/EirGrid/Annual-Renewable-Constraint-and-Curtailment-Report-2020.pdf>.
- [8] EirGrid and ESB, "Annual Electricity Transmission Performance Report 2020," URL: <https://www.eirgridgroup.com/site-files/library/EirGrid/Annual-Electricity-Transmission-Performance-Report-2020.pdf>.
- [9] S. Shrivastava, B. Subudhi, and S. Das, "Voltage and frequency synchronization of a low voltage inverter based microgrid," in *2017 4th International Conference on Power, Control & Embedded Systems (ICPCES)*. IEEE, 2017, pp. 1–6.
- [10] O. B. Adewuyi, R. Shigenobu, K. Ooya, T. Senjyu, and A. M. Howlader, "Static voltage stability improvement with battery energy storage considering optimal control of active and reactive power injection," *Electric Power Systems Research*, vol. 172, pp. 303–312, 2019.
- [11] W. Zhong, G. Tzounas, and F. Milano, "Improving the power system dynamic response through a combined voltage-frequency control of distributed energy resources," *IEEE Transactions on Power Systems*, pp. 1–1, 2022.
- [12] F. Milano, "A Python-based software tool for power system analysis," in *Proceedings of the IEEE PES General Meeting*, Jul. 2013, pp. 1–5.
- [13] —, *Power System Modelling and Scripting*. London: Springer, 2010.
- [14] V. Ajjarapu and B. Lee, "Bifurcation theory and its application to nonlinear dynamical phenomena in an electrical power system," *IEEE Transactions on Power Systems*, vol. 7, no. 1, pp. 424–431, 1992.
- [15] W. Zhong, M. A. A. Murad, M. Liu, and F. Milano, "Impact of virtual power plants on power system short-term transient response," *Electric Power Systems Research*, vol. 189, p. 106609, 2020.
- [16] F. P. Demello and C. Concordia, "Concepts of synchronous machine stability as affected by excitation control," *IEEE Transactions on power apparatus and systems*, vol. 88, no. 4, pp. 316–329, 1969.
- [17] C. Vournas, M. Pai, and P. Sauer, "The effect of automatic voltage regulation on the bifurcation evolution in power systems," *IEEE Transactions on Power Systems*, vol. 11, no. 4, pp. 1683–1688, 1996.